PCCP

Accepted Manuscript

ROYAL SOCIETY OF CHEMISTRY

www.rsc.org/pccp

Table of content entry

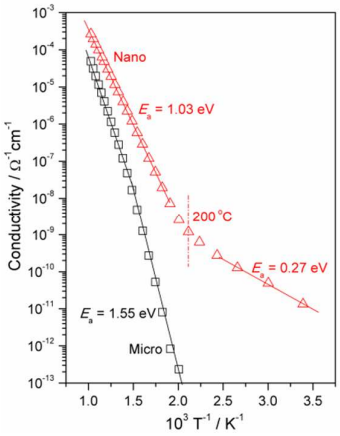

Only by decreasing grain size, one can transfer $BaTiO_3$ from an insulator to a semiconductor at room temperature.

PCCP

RSCPublishing

COMMUNICATION

Insulating-to-semiconducting transition in nanocrystalline $BaTiO_3$ at temperatures ≤ 200 °C

Cite this: DOI: 10.1039/x0xx00000x

Received ,
Accepted

DOI: 10.1039/x0xx00000x

www.rsc.org/

Xin Guo[a,b]*

As a classic dielectric material, $BaTiO_3$ is one of the most important materials used in electronic applications. In this work, highly dense $BaTiO_3$ ceramics with an average grain size of 35 nm were prepared, dielectric and electrical properties investigated. Microcrystalline $BaTiO_3$ is an insulator at low temperatures, however, nanocrystalline $BaTiO_3$ shows considerable semiconductivity with activation energy of only 0.27 eV at temperatures ≤ 200 °C. At room temperature, the conductivity of nanocrystalline $BaTiO_3$ is about fourteen orders of magnitude higher than that of microcrystalline counterpart. Only by decreasing grain size, one can transfer $BaTiO_3$ from an insulator to a semiconductor.

$BaTiO_3$ has been extensively used in the manufacture of multilayer ceramic capacitors (MLCC) that prevail in mobile electronic devices and personal computers;[1-3] nowadays the annual production of MLCC amounts to hundreds of billions pieces worldwide. In this sense, $BaTiO_3$ is the most important dielectric material used in electronic applications. Mobile electronic devices demand capacitors of high volumetric efficiency, i.e. high capacitance in small volume. To this end, the thickness of the dielectric layer is continuously decreasing; MLCC with a dielectric layer thickness of 2 μm have been commercialized, and those with a dielectric layer thickness of 0.1 μm have also been fabricated.[1,2] To further downsize MLCC, dielectric $BaTiO_3$ should become nanocrystalline.

From a scientific point of view, $BaTiO_3$ is an excellent model system for studying defect chemistry; the properties of microcrystalline $BaTiO_3$ have been demonstrated to clearly follow the basic principles of defect chemistry.[4] When the grain size decreases to the nanometre scale, materials usually exhibit a remarkable change in the transport properties.[5-8] One purpose of this work is to disclose the different defect thermodynamics of $BaTiO_3$ when the grain size decreases to the nanometre scale.

[a]*Laboratory of Solid State Ionics, School of Materials Science and Engineering, Huazhong University of Science and Technology, Wuhan 430074, P. R. China*
[b]*Peter Grünberg Institut, Forschungszentrum Jülich, 52425 Jülich, Germany*

In this work, highly dense $BaTiO_3$ ceramics with an average grain size of 35 nm were prepared, dielectric and electrical properties investigated. Microcrystalline $BaTiO_3$ is an insulator at low temperatures, however, nanocrystalline $BaTiO_3$ shows considerable semiconductivity with activation energy of only 0.27 eV at temperatures ≤ 200 °C.

Experimental

$BaTiO_3$ powder with an average particle diameter of ~10 nm was synthesized through the hydrolytic decomposition of a barium-titanium-isopropoxide solution in a water in oil microemulsion. The Ti/Ba ratio of the powder was determined to be 1.0035 ± 0.0004 by X-ray fluorescence spectroscopy. And according to inductively coupled plasma mass spectroscopy analyses, the $BaTiO_3$ powder was doped with acceptor impurities, mainly < 100 ppm Al, < 100 ppm Sc, < 8 ppm Cr, < 20 ppm Fe, < 25 ppm Mg, 82 ppm Mn, and < 12.8 ppm Ni. The consolidation of the powder was achieved by hot isostatic pressing under 200 MPa at 860 °C; the density of the ceramic pellets thus prepared was >93% of the theoretical density, and the average grain size 35 nm. For comparison, samples with an average grain size of 5.6 μm were prepared by firing the 35 nm grain samples at 1100 °C in air.

Platinum electrodes with a thickness of 200 nm were sputtered on both sides of the ceramic samples. The electrical properties were measured by impedance spectroscopy, performed at amplitude of 100 mV with a Solartron 1260 Frequency Response Analyzer, in conjunction with a 1296 Dielectric Interface. Impedance up to 10^{14} Ω can be reliably measured with the experimental setup. Experiments were conducted in pure oxygen ($pO_2 = 10^5$ Pa) over a temperature range of 23 to 700 °C, starting from 700 °C.

Results

As shown in Fig. 1, the nanocrystalline $BaTiO_3$ samples had very fine equiaxed grains with an average grain size of 35 nm, and the crystallographic grain boundaries (i.e. grain boundary cores) were atomically abrupt and free of any impurity phases. For comparison, samples with an average grain size of 5.6 μm were prepared by firing the nanocrystalline samples at 1100 °C in air. The different

sintering temperatures should result in quite different acceptor concentrations in nano- and microcrystalline $BaTiO_3$.

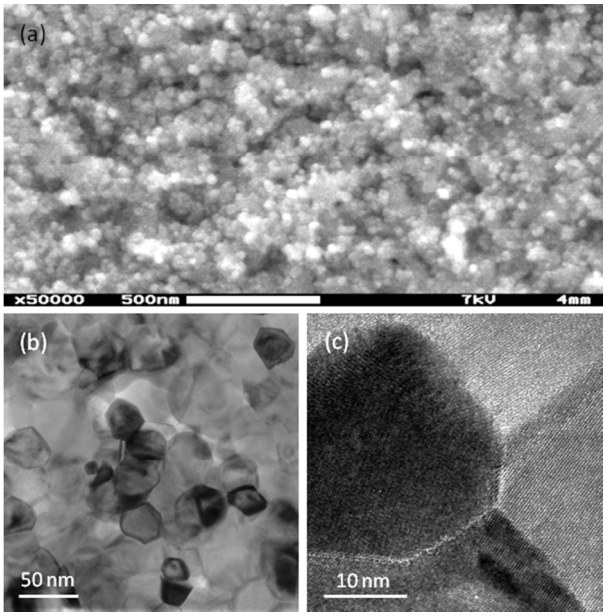

Fig. 1 (a) Scanning electron microscopy (SEM), (b) transmission electron microscopy (TEM) and (c) high-resolution transmission electron microscopy (HRTEM) images of nanocrystalline $BaTiO_3$ with an average grain size of 35 nm.

The electrical properties were measured by impedance spectroscopy. Experiments were conducted in pure oxygen ($pO_2 = 10^5$ Pa) over a temperature range of 23 to 700 °C, starting from 700 °C to ensure *p*-type conductivity. Although the experiments covered a broad temperature range, the focus of this work is on the properties of nanocrystalline $BaTiO_3$ determined at temperatures ≤ 200 °C. The high temperature properties were reported in previous works.[9,10]

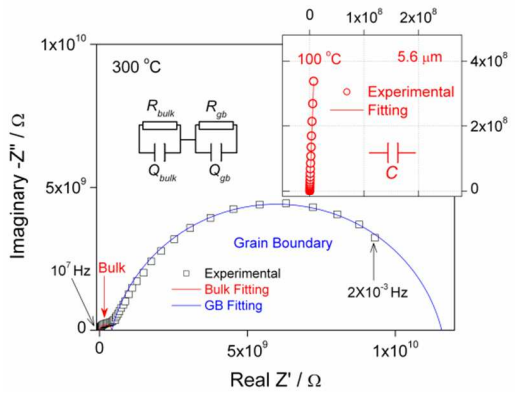

Fig. 2 Impedance spectra of $BaTiO_3$ with 5.6 μm grain size measured in oxygen at 100 and 300 °C, respectively. At 100 °C, microcrystalline $BaTiO_3$ shows only a capacitance effect.

Typical impedance spectra measured for the 5.6 μm grain size sample are presented in Fig. 2. Two well separated semicircles (relaxation processes) were recorded at temperatures ≥ 225 °C. In the order of decreasing frequency, the two semicircles correspond to the impedance responses of the grain bulk and the grain boundaries,[11] that of the electrodes is missing because the frequency was not low enough. The impedance spectra were then fitted according to an equivalent circuit consisting of two *RQ* circuits in series. Here *R* represents a resistance, *Q* a constant phase element, which is characterized by two parameters, C_Q and *n*. Corresponding capacitances *C* can be calculated from $C = (R^{1-n}C_Q)^{1/n}$. However, within the same frequency range, the microcrystalline sample shows only a capacitance effect at temperatures ≤ 200 °C (e.g. 100 °C), indicating that the resistance of the microcrystalline $BaTiO_3$ sample is $>>10^{14}$ Ω at such low temperatures.

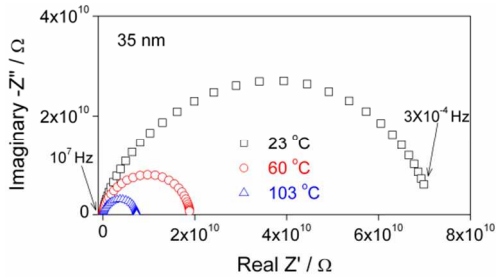

Fig. 3 Impedance spectra of $BaTiO_3$ with 35 nm grain size measured in oxygen at 23, 60 and 103 °C, respectively.

Only one distorted semicircle was recorded in the impedance spectrum of the 35 nm grain size sample within the whole experimental temperature range of 23 to 700 °C; Fig. 3 shows the impedance spectra at a few representative low temperatures. At such a small grain size, the relaxation time constants of the grain bulk and grain boundaries become similar. The distorted semicircle then results from the superposition of the contributions from the grain bulk and the grain boundaries; therefore, one cannot readily separate the grain bulk and grain boundary contributions in the 35 nm grain size sample. However, the intersection of the distorted semicircle on the real axis still gives the total resistance.

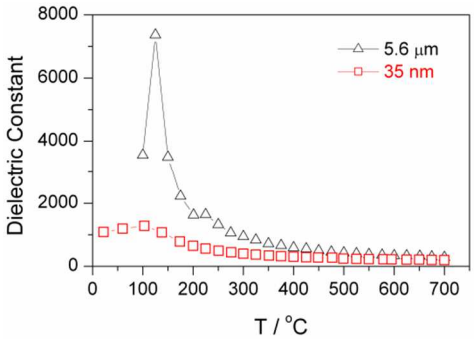

Fig. 4 Relative dielectric constants of nano- and microcrystalline $BaTiO_3$.

From the grain bulk capacitance of the 5.6 μm grain size sample, we calculated the dielectric constant; the results are given in Fig. 4. By fitting the dielectric constants according to the Curie-Weiss law, we obtained a Curie temperature of 130 °C, a very typical value for $BaTiO_3$ ceramics.[12,13] At the Curie temperature, the dielectric constant is almost as high as 8000, being consistent with the nature of an insulator.

Since it is not possible to derive the grain bulk capacitance from the impedance spectrum of the 35 nm grain size sample, the dielectric

constant of the nanocrystalline sample was determined from fixed frequency measurements at 100 kHz. It is a common practice to measure the dielectric constant at fixed frequencies,[12-14] typically 1 kHz, 10 kHz or 100 kHz. The dielectric constant of the 35 nm grain sample is also presented in Fig. 4 as a function of temperature. The dielectric constants of the micro- and nanocrystalline $BaTiO_3$ samples agree quite well with those reported in literatures.[13-17] At temperatures > 500 °C, the dielectric constants of both samples are quite similar, but at temperature ≤ 200 °C, the nanocrystalline sample has a significantly smaller dielectric constant.

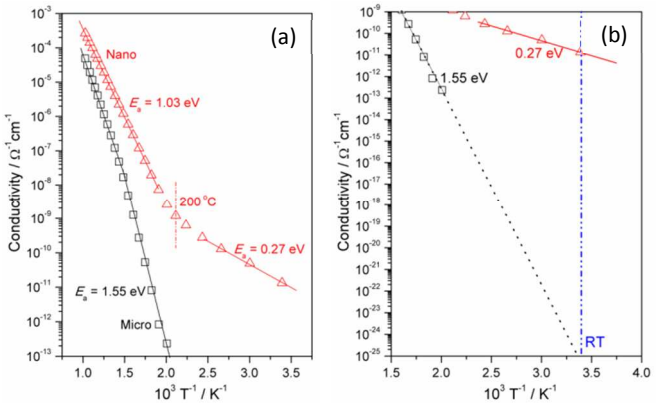

Fig. 5 Temperature dependence of the conductivities of nano- and microcrystalline $BaTiO_3$: (a) whole temperature range, and (b) low temperature range ≤ 200 °C.

The electrical conductivity can be calculated from $L/(R_{tot}A)$, here R_{tot} is the total resistance, L the sample thickness and A the cross-sectional area. Under intermediate to high oxygen partial pressure, acceptor-doped $BaTiO_3$ shows *p*-type conductivity.[4,18] The oxygen partial pressure dependence of the conductivity of nanocrystalline $BaTiO_3$ was checked and a 1/4 dependence was obtained,[9,10] corroborating the *p*-type conductivity. The *p*-type conductivities of the nano- and microcrystalline $BaTiO_3$ ceramics measured in oxygen are plotted in Fig. 5 as a function of temperature. At temperatures ≥ 500 °C, equilibrium conductivities were measured. However, a frozen-in situation appeared at low temperatures for kinetic reasons, therefore, non-equilibrium conductivities were obtained. Within the whole experimental temperature range, the conductivity of the 35 nm grain size sample is higher than that of the sample with 5.6 μm grain size. Compared with the conductivity of microcrystalline $BaTiO_3$ extrapolated to low temperatures (Fig. 5b), the conductivity of nanocrystalline $BaTiO_3$ is augmented by a factor as large as fourteen orders of magnitude at 23 °C. The activation energy for the conductivity of the microcrystalline $BaTiO_3$ is 1.55 eV, however, the activation energy for the conductivity of the nanocrystalline sample is distinctively smaller, and it decreases from 1.03 to 0.27 eV at temperatures around 200 °C.

Discussion

The dielectric properties of $BaTiO_3$ is usually described by a "core-shell" model;[12,13] in this model, the "core" is the ferroelectric grain bulk with a tetragonal structure, and the "shell" is the non-ferroelectric grain boundary (GB) layer with a pseudocubic structure. Such a GB layer is not necessarily a secondary phase, but a shell with disordered/defective structure close to the surface of the grains. The estimated thickness of the GB layer is comparable to the correlation length in ferroelectric perovskites (1-3 nm).[17] The dielectric constant of the $BaTiO_3$ grain bulk is on the scale of thousands, but the grain boundaries were suggested to have a temperature independent dielectric constant of only 130.[13] Since the GB portion increases with decreasing grain size, the decrease of grain size causes the progressive reduction of tetragonal distortion and dielectric constant; therefore, the dielectric constant of the nanocrystalline sample is significantly smaller than that of micro-crystalline one. According to a first-principle calculation,[19] a stress-free thin film of $BaTiO_3$ losses its ferroelectricity when the thickness is < ~3.6 nm.

The *p*-type conductivity is due to excess holes in $BaTiO_3$, and holes are produced by the oxidation reaction at high temperatures

$$V_O^{\bullet\bullet} + 1/2\,O_2 \rightleftharpoons O_O^{\times} + 2h^{\bullet} \quad (1a)$$

$$K_{Ox}(T) = \frac{[O_O^{\times}]\,p^2}{[V_O^{\bullet\bullet}]}\,pO_2^{-1/2} = K_{Ox}^0 \exp\left(-\frac{\Delta H_{Ox}}{k_B T}\right) \quad (1b)$$

The equations follow the Kröger-Vink notation. In Eq. (1b), K_{Ox}^0 is the pre-exponential constant, $[V_O^{\bullet\bullet}]$ the concentration of oxygen vacancies, ΔH_{Ox} the oxidation enthalpy, and it was determined to be 0.92 eV for microcrystalline $BaTiO_3$.[4] The 35 nm and 5.6 μm grain size samples were annealed at 700 °C and under pO_2 = 2 Pa for 30 hours, afterwards, pure oxygen was introduced and both samples were annealed in oxygen for another 30 hours. This treatment caused a mass gain of 0.023 wt.% in the microcrystalline sample, whereas 0.098 wt.% in the nanocrystalline one. The annealing in oxygen caused an oxygen excess of δ; the δ value is directly related to the mass gain. Assuming that K_{Ox}^0 does not change with grain size, a ΔH_{Ox} decrease of ~0.3 eV in the nanocrystalline sample can be determined from the difference in the mass gain. Furthermore, from the activation energy difference shown in Fig. 5a, one can also expect a significant decrease in ΔH_{Ox} for nanocrystalline $BaTiO_3$. In view of the very different electrical and dielectric properties of the grain boundaries and a greater degree of disorder at the grain boundaries, it is reasonable to expect different defect thermo-dynamics at the grain boundaries. The grain boundaries of extremely high density in nanocrystalline $BaTiO_3$ facilitate the oxidation reaction, and thus decrease ΔH_{Ox}.

The maximal acceptor concentration in the samples is ~3×10^{19} cm^{-3}. From the defect chemistry of $BaTiO_3$,[4,18] the hole concentration in the 5.6 μm grain size sample can be calculated to be ~3×10^{18} cm^{-3} at 700 °C and under an oxygen partial pressure of 10^5 Pa. The remarkable reduction of the oxidation enthalpy enhances the hole concentration in the 35 nm grain size sample by a factor of ~10, agreeing well with the higher conductivity of the nanocrystalline sample.

Holes can be trapped by acceptors, the trapping reaction is[4,20,21]

$$A^{\times} \rightleftharpoons A' + h^{\bullet} \quad (2a)$$

$$K_A(T) = \frac{[A']\,p}{[A^{\times}]} = K_A^0 \exp\left(-\frac{\Delta H_A}{k_B T}\right) \quad (2b)$$

In Eq. (2b), K_A^0 is the pre-exponential constant, ΔH_A the trapping enthalpy of holes, and it was determined to be 0.54 eV for undoped,[4]

and 1.04 eV for Al-doped $BaTiO_3$ ceramics.[20] Holes can be trapped by acceptors, and trapped holes can also be released; there exists a trapping/releasing equilibrium. Once a trapped hole is released, it also contributes to the electrical conduction. The lifetime of $A^{\times}$ is short at high temperatures (e.g. >800 °C), but increases significantly with decreasing temperature.[21] At low temperatures, acceptors become deep traps for holes, then the lifetime of trapped holes is infinitely long; in this circumstance, the trapped holes make no contribution to the electrical conduction.

Although assuming an equilibrium situation is unrealistic for $BaTiO_3$ at low temperatures, the equilibrium hole concentration was still calculated here to get a feeling of the trapping effect of acceptors. The defect chemistry calculation gives a hole concentration of $\sim 10^{13}$ cm^{-3} in the 5.6 μm grain size sample at 225 °C and under an oxygen partial pressure of 10^5 Pa. But the free holes, those who are not trapped to acceptors and therefore contribute to the *p*-type conductivity, have a concentration of only $\sim 8\times 10^8$ cm^{-3}, when calculated from the bulk conductivity at 225 °C. This indicates an amazing trapping effect. Since $\left[A'\right] > p$ in microcrystalline $BaTiO_3$, almost all holes can be trapped to acceptors at low temperatures (e.g. ≤ 200 °C); therefore, the 5.6 μm grain sample becomes insulating.

Acceptor-type impurities were present in the powder. Owing to the lower sintering temperature (860 °C), the concentration of dissolved acceptors in the nanocrystalline sample was lower. The remarkably smaller oxidation enthalpy indicates that the defect thermodynamics of nanocrystalline $BaTiO_3$ is different; one might also expect a smaller trapping enthalpy. In addition, the hole concentration in the 35 nm grain size sample was substantially higher. As a result of the lower acceptor concentration, smaller trapping enthalpy and higher hole concentration, free holes could never be exhausted in nanocrystalline $BaTiO_3$ even at room temperature.

In view of Eqs. (1) and (2), the oxidation enthalpy ΔH_{Ox} and the trapping enthalpy ΔH_{A} should be the vital components of the activation energy for the *p*-type conductivity, in addition to the migration enthalpy of holes ΔH_m. At temperatures ≤ 200 °C, the oxidation reaction is kinetically much too sluggish, and most of holes are deeply trapped to acceptors, making no contribution to the electrical conduction; excess free holes are the only mobile charge carriers. Under this condition, the activation energy essentially decreases to only the migration enthalpy. From Fig. 5, we know that the migration enthalpy is 0.27 eV at temperatures ≤ 200 °C.

Conclusion

$BaTiO_3$ shows a different defect thermodynamics at nanometre scale, which is reflected by the reduced oxidation enthalpy of nanocrystalline $BaTiO_3$. Therefore, the hole concentration of nanocrystalline $BaTiO_3$ is significantly higher than that of micro-crystalline counterpart, and nanocrystalline $BaTiO_3$ shows considerable semiconductivity at temperatures ≤ 200 °C.

Acknowledgements

C. Ohly of Bosch is appreciated for providing the nanocrystalline sample, and S. Mi of Institute of Metals, CAS, for performing the TEM observation.

References

1 H. Kishi, Y. Mizuno, H. Chazono, *Jpn. J. Appl. Phys.*, 2003, **42**, 1-15.
2 C. Pithan, D. Hennings, R. Waser, *Int. J. Appl. Ceram. Technol.*, 2005, **2**, 1-14.
3 C. A. Randall, *J. Ceram. Soc. Jpn.*, 2001, **109**, S2-S6.
4 D. M. Smyth, *The Defect Chemistry of Metal Oxides*, Oxford University Press, Oxford, 2000, p.253-282.
5 J. Maier, *Prog. Solid State Chem.*, 1995, **23**, 171-263.
6 J. Maier, *Nature Mater.*, 2005, **4**, 805-815.
7 J. Maier, *Adv. Mater.*, 2009, **21,** 2571-2585.
8 N. Sata, K. Eberman, K. Eberl, J. Maier, *Nature*, 2000, **408**, 946-949.
9 X. Guo, et al. *Appl. Phys. Lett.*, 2005, **86**, 082110.
10 X. Guo, *Acta Mater.*, 2013, **61**, 1748-1756.
11 N. Hirose, A. R. West, *J. Am. Ceram. Soc.*, 1996, **79**, 1633-1641.
12 G. Arlt, D. Hennings, G. de With, *J. Appl. Phys.*, 1985, **58**, 1619-1625.
13 M. H. Frey, Z. Xu, P. Han, D. A. Payne, *Ferroelectrics*, 1998, **206-207**, 337-353.
14 X. Deng, et al. *Appl. Phys. Lett.*, 2006, **88**, 252905.
15 X. Wang, X. Deng, H. Wen, L. Li, *Appl. Phys. Lett.*, 2006, **89**, 162902.
16 L. Mitoseriu, et al. *Appl. Phys. Lett.*, 2004, **84**, 2418-2420.
17 M. T. Buscaglia, et al. *Phys. Rew. B*, 2006, **73**, 064114.
18 H.-I. Yoo, C.-R. Song, D.-K. Lee, *J. Electroceram.*, 2002, **8**, 5-36.
19 M. G. Stachiotti, *Appl. Phys. Lett.*, 2004, **94**, 251.
20 H.-I. Yoo, *Proceedings of the 26th RisØ International Symposium on Materials Science: Solid State Chemistry*, Eds. S. Linderoth, A. Smith, N. Bonanos, A. Hagen, L. Mikkelsen, K. Kammer, D. Lybye, P. V. Hendriksen, F. W. Poulsen, M. Mogensen, W. G. Wang, RisØ National Laboratory, Roskilde, Denmark, 2005, p.89-106.
21 M. Martin, *Phys. Chem. Chem. Phys.*, 2004, **6**, 3627-3632.

